Journal of Crystal Growth 416 (2015) 8–11

Contents lists available at ScienceDirect

Journal of Crystal Growth

journal homepage: www.elsevier.com/locate/jcrysgro

# Coincident site lattice bi-crystals growth—Impurity segregation towards grain boundaries

ARTICLE INFO

*Keywords:*
A1. Grain boundaries
A1. Impurities
A1. Segregation
Multicrystalline silicon
Seeded growth

ABSTRACT

Bi-crystal silicon ingots with coincident site lattice (CSL) grain boundaries (GB), namely Σ3, Σ9, Σ27a, have been grown in a small scale Bridgman type furnace at 3 μm/s. Melts have been intentionally polluted with 25 ppma of copper and indium. Segregation of these impurities towards the central grain boundaries has been assessed by secondary ion mass spectrometry (SIMS). Influence of topological imperfections and grain boundary nature has been investigated. While copper segregation towards Σ3 GB has not been detected, copper has been found to diffuse towards Σ9 and Σ27a GB, especially at steps and GB junctions. Indium segregation has not been detected at any GB. This indicates that slow-diffusing element segregation towards GB depends on the boundary nature, and/or the grains orientation.



## 1. Introduction

Multicrystalline silicon based solar cells performance is affected by a wide range of impurities. It has been shown that transition metals, even at very low concentrations, drastically decrease solar cells efficiencies [1]. These impurities are distributed inhomogeneously in the material, as they tend to be gettered at defects such as grain boundaries [2,3]. Slow diffusing elements have also been observed to segregate at grain boundaries during multicrystalline silicon solidification [4,5]. Impurity segregation at defects has been identified as the origin of grain boundaries' electrical activity [6,7] and impacts the bulk carrier recombination [8]. Therefore, a fundamental understanding of grain boundary segregation in silicon is of main importance to improve solar cells energy conversion efficiency.

Different types of grain boundaries are found in multicrystalline silicon. Coincident site lattice type of grain boundaries are the most common ones—especially in Σ3, Σ9 and Σ27 configurations. Previous studies in multicrystalline silicon report between 22% and 64% of Σ3 grain boundaries, between 9% and 12% of Σ9 and between 3% and 9% of Σ27 [9–11]. These grain boundaries form junctions and topological imperfections such as kinks and steps.

In this study, bi-crystals separated by selected coincident site lattice grain boundaries – i.e. Σ3, Σ9 and Σ27a – have been solidified using the seeded-growth method in a Bridgman type furnace. Copper, which is a common fast diffusing element in solid silicon, and indium, which is a less common slow-diffusing element in solid silicon, were added to the melt. Their distributions around the central grain boundaries have been analyzed by secondary ion mass spectrometry (SIMS). The impact of grain boundary topological imperfections has been assessed.

## 2. Experimental set up and method

Cylindrical silicon bi-crystals (32 mm diameter and ~100 g weight) separated by coincident site lattice (CSL) grain boundaries have been solidified in a Bridgman type furnace by using the seeded-growth method. The melts have been intentionally contaminated with 25 ppma of copper and 25 ppma of indium. More details about the solidification method are given in Ref. [4,12]. Monocrystalline seeds have been prepared from Czochralski ingots and are oriented in ⟨1 1 0⟩ direction. Detailed seed preparation method is given in Ref. [12]. The pulling rate was 3 μm/s, corresponding to the lowest speed in Ref. [4].

2 mm thick horizontal slices of have been cut 5 mm above the seeds. Samples have been polished down to 1 μm, and defects have been revealed by Sopori etchant. Chemical analyses have been performed by secondary ion mass spectrometry (SIMS) after cleaning the samples with fluoric acid and ethanol. 8 μm spots have been used for local analyses—i.e. same size that the one used in Ref. [4]. The values provided here are averages of measurements made between 4 μm and 7 μm depths. Copper bulk content analyses have been performed by glow discharge mass spectrometry (GDMS) as well. Grain boundaries nature and planes identification has been performed by electron back scattered diffraction (EBSD).

## 3. Results and discussion

The structure development of the grown CSL grain boundaries is described in Ref. [12]. It is shown that the Σ9 and Σ27a seed grain boundaries have a tendency to rearrange during the growth, forming topological imperfections—i.e. steps mainly. In the present study, local SIMS analyses have been performed at different positions along the grain boundaries. Positions at segments of low energy configurations and at topological imperfections have been selected. Despite the intentional pollution of the melt, indium and copper are present in the ingots as traces. The interactions between the two elements are therefore expected to be negligible.

### 3.1. Indium analyses

Indium analyses have been performed at the grown $\Sigma 3\{1\,1\,1\}_{1,2}$ grain boundary and at segments of low energy configuration at the grown Σ9 and Σ27a grain boundaries. The low energy

http://dx.doi.org/10.1016/j.jcrysgro.2015.01.009
0022-0248/

configurations of the selected segments were $\Sigma 9\{2\,2\,1\}_{1,2}$ and $\Sigma 27a\{5\,1\,1\}_{1,2}$, respectively.

In a previous work [4], the authors have added 50 ppma indium to the melt, i.e. twice that of the present study, and 5° small angle grain boundaries were studied. The content at the slowly grown sub-grain boundary has been found to be $1.7\times10^{16}$ cm$^{-3}$. By using the same analysis parameters and the same instrument than the one used in Ref. [4], the In concentration at the grain boundaries has been found to be below the detection limit—i.e. $\sim4\times10^{14}$ cm$^{-3}$, for all $\Sigma 3$, $\Sigma 9\{2\,2\,1\}_{1,2}$ and $\Sigma 27a\{5\,1\,1\}_{1,2}$ grain boundaries. It can be stated that indium has segregated less at CSL grain boundaries, than at the sub-grain boundary. In fact, if indium would have segregated as efficiently at the CSL as at the sub-grain boundary, a concentration of $\sim8\times10^{15}$ cm$^{-3}$ would have been measured. The absence of indium segregation at the CSL grain boundaries is a consequence of (1) grain boundary nature and/or (2) seed orientation.

(1) Indium has a very low diffusivity in solid silicon (at the melting temperature, indium diffusivity in solid silicon is $3\times10^{-11}$ cm$^2$/s [13]). Therefore, it does not segregate at grain boundaries by diffusion in the solid. The solubility of impurities in solid silicon has been found to be higher at grain boundaries than in the bulk [5,14]. In Ref. [4,5], it is argued that the relative higher solubility of impurities at grain boundaries can explain the segregation of slowly diffusing impurities such as indium at grain boundaries, as a consequence of their limited rejection at the solid–liquid interface during the growth. Impurity solubility at grain boundaries can be expected to be dependant on the grain boundary nature as the density of sites for impurities depends on the atomic arrangement of the boundary interface.

(2) The crystal–melt interface morphology, at the grain–grain–liquid triple phase line, is described by Duffar et al. [15]. Recent investigations made by X-ray radiography imaging and light microscopy in-situ observations have shown the formation of a groove at this triple line, with the exception of $\Sigma 3$ grain boundaries [16,17]. It has been suggested by Fujiwara et al. that this local morphology could locally enrich the melt in the groove, as a result of a "2 dimensional" impurity rejection occurring at the grain–grain–liquid triple line [17]. This local melt enrichment would have a direct influence on the content of impurities in the solid at the grain boundary, and could explain the segregation of slowly diffusing impurities. In the work made by Tandjaoui et al., the grooves have been found to be bounded by either rough faces or {1 1 1} facets [16]. In the case of a faceted groove, the shape and narrowness of the groove is directly related to the seed orientation, as sketched in Fig. 1. In Ref. [4], seeds oriented in ⟨1 0 0⟩ were used. In the present study, seeds were oriented in the ⟨1 1 0⟩ direction. The angle between the two facets bounding the groove would then be ~110°, as compared to ~70° for ⟨1 0 0⟩ seeds. This would limit the impact of the "2 dimensional" impurity rejection suggested by Fujiwara et al., as the groove is more open towards the melt and re-mixing through natural convection is facilitated. In addition, the coherency of the grain boundary segments analyzed in this study are believed to be relatively high as they have rearranged during the growth to approach low energy configurations [12], contrary to the sub-grain boundaries studied in Ref. [4] which are incoherent. The grain boundary coherency affects its tendency of faceting. Fujiwara et al. observed no facets at $\Sigma 3$ grain boundaries [17], as a result of their high degree of coherency and therefore low interfacial energy. Facets are less likely to appear at CSL grain boundaries, especially those with high density of coincident site—i.e. low $\Sigma$ values.

### 3.2. Copper analyses

The grain boundaries structure developments are shown in Fig. 2, and described in Ref. [12]. Re-arrangements of the grain boundaries towards low energy configurations introduce topological

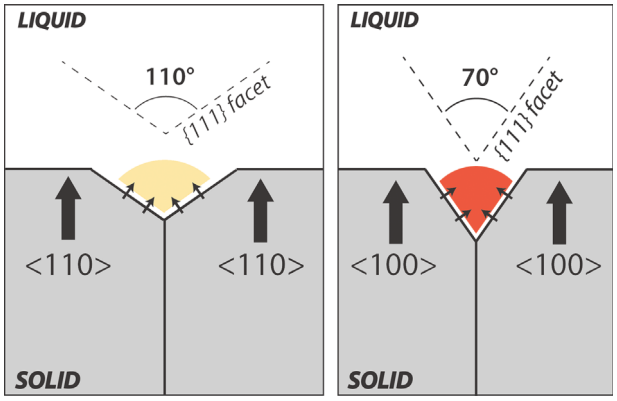


**Fig. 1.** Grain–grain–liquid triple phase line facetted groove morphology for seeds oriented in ⟨1 1 0⟩ direction (left) and ⟨1 0 0⟩ direction (right).

imperfections such as steps. The $\Sigma 9$ grain boundary has also been observed to locally dissociate into two $\Sigma 3$ grain boundaries. Local SIMS analyses have been performed at the positions shown on Fig. 2, and are listed in Table 1. No copper has been detected at the central grain boundary of the $\Sigma 3$ bi-crystal. The bulk concentrations, obtained by GDMS analyses, are also reported.

Table 1 shows a more pronounced average segregation of copper towards the $\Sigma 27a$ grain boundary, in comparison to the $\Sigma 9$ grain boundary—$C_{Cu}/C_{bulk}=21$ for $\Sigma 27a$ vs. 6.6 for $\Sigma 9$. In multicrystalline silicon, copper segregates towards grain boundaries by solid state diffusion [4,12]. Trapping of impurity atoms at boundaries is described by Myers et al. [18]. The segregation intensity is related to the impurity concentration in the matrix, temperature history and the Gibbs energy of segregation $\Delta G_s$. The temperature history is identical for both $\Sigma 9$ and $\Sigma 27a$ bi-crystals, and the concentration in the matrix is comparable (see $C_{bulk}$ in Table 1). This suggests that the free energy of segregation of copper at $\Sigma 27a$ grain boundary is on average lower than its free energy of segregation at $\Sigma 9$. Impurity segregation towards grain boundary is mainly driven by elastic interaction between the matrix and the impurity atoms, as the solute and the matrix do not occupy the same molar volume, and do not have the same elasticity. Once the solute atom has segregated at the grain boundary, a relaxation occurs, and the energy of the system decreases. This includes grain boundary relaxation, which amplitude can be expected to depend on the original interfacial energy of the boundary. Even if some exceptions can be found in literature – e.g. $\Sigma 59$ has lower interfacial energy than $\Sigma 11$ and $\Sigma 33$ in silicon [19] – CSL grain boundaries interfacial energies are usually considered to be dependant on their density of coincident site: a high density – i.e. low $\Sigma$ value – corresponds to a low interfacial energy [20]. Kohyama et al. have calculated a lower interfacial energy of $\Sigma 3$ relatively to $\Sigma 9$ which has a lower interfacial energy relatively to $\Sigma 27a$ in silicon [19]. In addition, an interfacial energy close to 0 J/m$^2$ has been reported for symmetric $\Sigma 3\{1\,1\,1\}$ grain boundaries [19–22], explaining the non-detection of copper at the central grain boundary of the $\Sigma 3$ bi-crystal.

Copper analyses were performed at the topological imperfection points present at $\Sigma 9$ and $\Sigma 27a$ grain boundaries (see Fig. 2), in order to study segregation along grain boundaries. Analyses made at the central grain boundary of the $\Sigma 9$ bi-crystal show a more pronounced segregation of copper at the junction between the $\Sigma 9$ and the two $\Sigma 3$ resulting from the local $\Sigma 9$ dissociation—$C_{junction}/C_{\Sigma 9}=4.1$ (see Fig. 2 and Table 1). Nordmark et al. performed electron-beam-induced current (EBIC), EBSD and transmission electron microscopy (TEM) studies on multicrystalline silicon obtained from metallurgical grade silicon and observed that metallic silicide precipitates are very common at triple points—i.e. junction between three grains [23]. The present study suggests that these observations are the result of a local high segregation at triple points. Similarly, at the central grain